

# LINAC OPTICS OPTIMIZATION WITH MULTI-OBJECTIVE OPTIMIZATION\*

I. Neththikumara<sup>†1</sup>, T. Satogata<sup>1,2</sup>, S.A. Bogacz<sup>2</sup>, R.M. Bodenstein<sup>2</sup>, and A. Vandenhoeke<sup>3</sup>  
<sup>1</sup>Old Dominion University, Norfolk, USA  
<sup>2</sup>Jefferson Lab., Newport News, USA  
<sup>3</sup>Artificial Intelligence Lab, Brussels, Belgium

## Abstract

The beamline design of recirculating linacs requires special attention to avoid beam instabilities due to RF wakefields. A proposed high-energy, multi-pass energy recovery demonstration at CEBAF uses a low beam current. Stronger focusing at lower energies is necessary to avoid beam breakup (BBU) instabilities, even with this small beam current. The CEBAF linac optics optimization balances over-focusing at higher energies and beta excursions at lower energies. Using proper mathematical expressions, linac optics optimization can be achieved with evolutionary algorithms. Here, we present the optimization process of North Linac optics using multi-objective optimization.

## INTRODUCTION

A multi-pass energy recovery (ER) experiment proposed at Jefferson Lab's CEBAF accelerator uses a high-energy electron beam. This aims to explore a new regime in ER history, an efficient energy recovery of electrons in the presence of substantial incoherent synchrotron radiation (ISR) [1].

Two superconducting linacs, connected by five vertically stacked arcs at both sides, make up the racetrack shape of CEBAF. Electron bunches accelerate on RF crest through eleven linac passes up to 12 GeV; these bunches are used and dumped at any or all of four experimental halls at intermediate energies.

Reuse of the RF energy of the accelerated beam increases the overall efficiency of the RF system. ER capability can be incorporated into CEBAF with the addition of a new path length chicane, adding a path length of  $\lambda_{rf}/2$  after the fifth accelerating pass. This would shift bunches into the R minima, and would allow the transfer of their energy back to RF during deceleration. After five decelerating passes bunches would be dumped at a low energy dump at the end of the South Linac (SL). A schematic of the proposed modifications is shown in Figure 1. The additional chicane and dump will not affect routine CEBAF operations.

## MULTIPASS LINAC OPTICS

ERLs with racetrack topology require that both accelerating and decelerating beams share the same arcs corresponding to their energy. This requirement imposes a specific constraint in Twiss functions at the linac ends. Linac-end

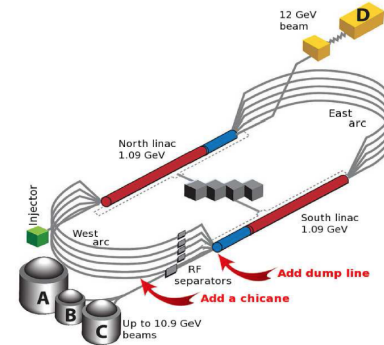


Figure 1: CEBAF accelerator, with arrows indicating new hardware installation sites.

Twiss values must be identical for both accelerating/decelerating passes that share an arc. The work presented here will focus on North Linac (NL) studies, where ten total passes (five accelerating and five decelerating) will pass through the linac. For these simulations, the accelerating beam uses the beamline elements as they are normally arranged. Decelerating bunches pass through the elements in reversed order. Graphically, the accelerating and decelerating passes are alternately connected at places of equal energy with a special matrix,  $M$ , to match with arc-end optics as illustrated in Figure 2. Here, blue arrows denote accelerating linac optics and red arrows denote decelerating linac optics. At

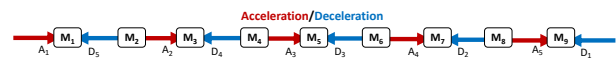


Figure 2: 10 pass beamline arrangement [2].

For this study, the 13-FODO-cell CEBAF NL lattice is considered. A previous, manual optimization is shown in Figure 3, for a symmetric FODO-like layout with  $60^\circ$  phase advance per cell.

In recirculating linacs, beam break-up (BBU) instabilities limit the threshold beam current,  $I_{th}$  [3]. For a single pill box cavity in  $TM_{00}$  mode,  $I_{th}$  is given as,

$$I_{th} = \frac{2pc}{e\omega Q \frac{R}{Q}} \frac{1}{|T_{12}| \sin \omega T_{tr}} \quad (1)$$

Here,  $Q$  is the cavity quality factor,  $\frac{p}{e}$  is beam rigidity,  $\omega$  is the HOM angular frequency, and  $|T_{tr}|$  is the transfer matrix

\* This material is based upon work supported by the U.S. Department of Energy under contract DE-AC05-06OR23177.

<sup>†</sup> ineth001@odu.edu

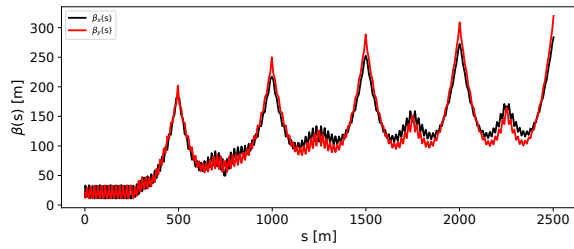


Figure 3: Multipass optics for 60 degree FODO-like linac.

element that measures the beam centroid displacement at the second pass from an initial kick. Equation 1 can be reduced to the following, where minimizing the average value suppresses BBU in recirculating linacs. [4]:

$$\left\langle \frac{\beta}{E} \right\rangle = \int \left( \frac{\beta}{E} \right) ds \quad (2)$$

According to Equation 2, the  $\beta$  values at lower energies need to be much smaller than the  $\beta$  values at higher energies. The optimized solution given in Figure 3 has smaller, tighter  $\beta$  variations at the first pass. Mirror symmetric  $\beta$  variation is not clearly visible here, but it is a requirement for the design due to arc sharing. Higher pass  $\beta$  variations need to be controlled by minimizing the differences at the linac end  $\beta$  values.

At the end of the beamline,  $\beta$  function values should be closer to the length of the linac. For the NL, this value needs to be less than 300 m.

The optics requirements are met by adjusting the quadrupole focusing in the linac. Performing this action manually takes a considerable amount of time, as there are multiple objectives to consider. Hence, this study focuses on multi-objective optimization with evolutionary algorithms.

## EVOLUTIONARY ALGORITHMS

Evolutionary algorithms (EAs) are used to capture an optimum solution or a set of solutions for single or multi-objective search problems and no gradient information is required in the problem definition. Genetic algorithms (GA) are a powerful metaheuristic class of EAs, with three main operators; *selection*, *crossover* and *mutation* [5]. Solutions are a set of vectors referred to as *chromosomes* made out of *genes*. GAs represent them as an evolving population of individuals following the survival of the fittest.

In this work, to handle multiobjectives, we consider Non-dominated Sorting Genetic Algorithm (NSGA II) [6] in the problem implementation within a python framework [7].

### Definition of the Multi-Objective Optimization Problem

The optimization of the 10-pass NL optics involves minimization of multiple conflicting objectives [8]. Without loss of generality, the multi-objective minimization problem is

defined as, [9]:

$$\begin{aligned} & \text{Minimize } F(x) = [F_1(x), F_2(x), \dots, F_k(x)]^T \\ & \text{subject to } g_j(x) \leq 0, \quad j = 1, 2, \dots, m \\ & h_l(x) = 0, \quad l = 1, 2, \dots, e \end{aligned} \quad (3)$$

Here,  $k$ ,  $m$ , and  $e$  refer to the number of objective functions, inequality constraints, and equality constraints, respectively. Generally, optimization of all objectives cannot be done simultaneously, hence a set of solutions is obtained that fit a predetermined definition for an optimality [9]. The set of Pareto optimal solutions is called the *Pareto optimal set*, for which the corresponding objective functions in the objective space form the *Pareto front*. Our goal here is to define a multi-objective optimization algorithm to compute the best known Pareto front, that is ideally be close to the true front.

## OBJECTIVE DEFINITION

Multipass linac optics optimization involve two main objectives: minimization of lower energy  $\beta$  fluctuation, and controlling the  $\beta$  peaks with mirror-symmetric variation.

Here, there are 30 variables in the problem; 26 quadrupole fields, and 4 initial Twiss values. Carrying out a 30-variable search is complex without recognizing the appropriate search space. Therefore, the problem was set up as a study with increasing variables. Initial tests for this search were carried out with two-objectives up to 10 variables [10]. It was observed that increasing the search space lowered the effectiveness of the objectives defined, necessitating the definition of a new set of objectives to complete 30-dimensional search problem.

This study includes three objectives. The first one focuses on minimization of the differences in  $\beta$  values at each element in  $x$  and  $y$  planes. For this, moving averages (MA) of  $\beta_x$  and  $\beta_y$  are calculated. The window size for this calculation was obtained by analyzing the outcomes of the MA. Then, taking the mean squared error (MSE) of these MAs, the first objective function is defined as following.

$$\text{Function 1 (F}_1\text{)} = \text{MSE}[MA(\beta_x), MA(\beta_y)] \quad (4)$$

In the second objective, minimization of peak  $\beta$  values in each pass is done by calculating the average of the peak values in 10-passes. To couple  $x$  and  $y$  planes, the geometric mean of these values are used as follows:

$$\text{Function 2 (F}_2\text{)} = \left( \prod_{i=x,y} \left[ \frac{1}{n} \sum_{i=1}^n \beta_{i-\max} \right] \right)^{\frac{1}{2}} \quad (5)$$

The third objective is to control the differences in the peak  $\beta$  values for each pass. Prior experiences suggested that these peak differences need to be controlled with an additional objective function. Otherwise, suppression of peak beta values tends to make linac end  $\beta$  be at a minima, destroying the symmetry of this lattice optics. Only the 2<sup>nd</sup>, 3<sup>rd</sup>, 4<sup>th</sup>, and 5<sup>th</sup> passes tend to show this abnormal behaviour. To ensure the  $\beta$  peaks ( $\beta_{i-\max}$ ) at the end of

each pass, the third objective function is defined coupling x and y planes as before.

$$\text{Function 3 } (F_3) = \prod_{i=x,y} \left( \sum_{i=2}^5 |\beta_{i-\max} - \beta_{i+1-\max}| \right)^{\frac{1}{2}} \quad (6)$$

Along with these objectives, two constraints are required to control the first pass peak  $\beta$  values:

$$C_{1,2} = \beta_{(x,y), \max}^{1st \text{ pass}} - 60 \text{ m} \quad (7)$$

## RESULTS AND DISCUSSION

Optimization of 10-pass NL lattice optics involves adjusting 26 quadrupole fields (L02-L27), along with initial Twiss values. Reduction of the required computational time is a challenge in this optimization study.

### Magnetic Field Variations

Solutions for the 30-variables were obtained by systematically increasing the variable numbers, population size, and generation number. Outputs of the Pareto front solutions were analyzed, and according to the outcomes, adjustments were made to the population size and number of generations. One difficulty with this approach proved to be the large computational time required.

The individual lattice settings obtained in the 30-variable search Pareto front were used in this study. Analysis of the quadrupole field variation of the Pareto optimal set is represented with box plots, and is shown in Fig. 4.

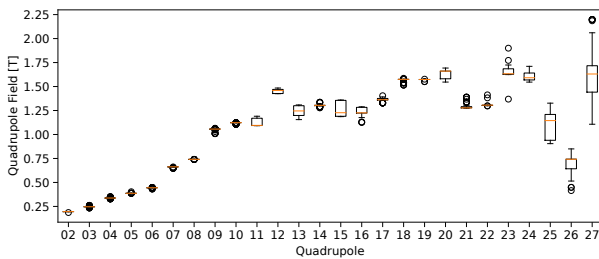


Figure 4: Magnetic field variations in Pareto front individuals for N=500, gen. no=200.

Figure 4 shows the variations of the 26 quadrupole fields. Most of the quadrupoles do not have a large variation, and the upper and lower bounds for these magnets used to reduce the search space. This reduction allowed for use of a smaller population, which lowered the generation number, and decreased the computational time.

### 30-Variable Search Results

With the redefined parameters, a 30-variable search was performed for different numbers of generation with a population size of 500. The Pareto fronts obtained for different generations are given in Figure 5. This shows that the Pareto front converges as the generation number increases. The 225 generation search concluded with 42 individuals, whereas

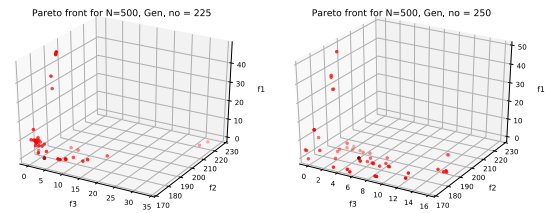


Figure 5: Resulted Pareto fronts for N=500 with generations 225 and 250.

the 250 generation search ended with 51 solutions. Improvement of the optics is observed with the comparison of optics of Pareto front individuals. Figure 6 illustrates the optics of

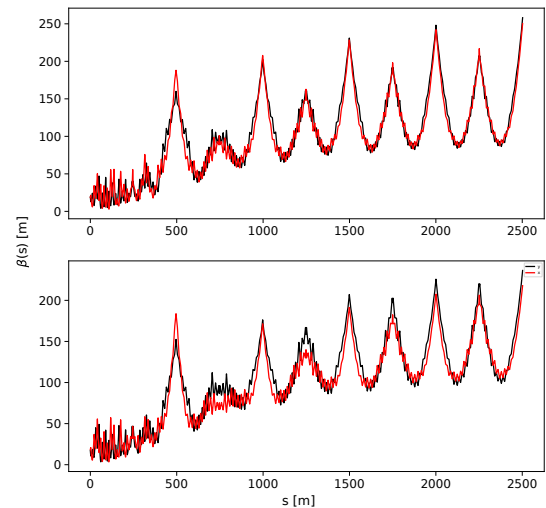


Figure 6: Optics of two best solutions from different searches.

glance, both the solutions look similar, but there are some slight differences in between them. Mirror symmetry in the higher passes is preserved in the 225 generation case (top), whereas the end values at the 2<sup>nd</sup> pass goes to a minima there. The 250 generation case (bottom) shows lower peak values at the 2<sup>nd</sup> pass. Determining the “best” solution without compromising both requirements is non-trivial. Both of the solutions for lattice settings obtained with these MOO-EA search are acceptable.

## CONCLUSIONS AND FUTURE WORK

Optics comparison of the Pareto front individuals of search with 225 generations and 250 generations show the proper mirror-symmetry  $\beta$  variation for higher passes. The first pass  $\beta$  values vary with a maximum of 60 m, within the constraints. The required population size can be reduced by limiting the search space, leading to a reduction of computational time.

This optimized solution will be used for both the North Linac and South Linac lattices. Using the optics from these optimized lattices, the recirculating arcs can be re-scaled to

match. Ultimately, a 10-pass beamline for ER@CEBAF can be designed.

## REFERENCES

- [1] S.A. Bogacz *et. al.*, “ER@CEBAF: A test of 5-pass energy recovery at CEBAF”, Collider-Accelerator Department, Brookhaven National Laboratory, 2016.
- [2] I. Neththikumara, T. Satogata, S.A. Bogacz, R.M. Bodenstein, A. Vandenhoeke, “Lattice Optics Optimization for Recirculating Energy Recovery Linacs with Multi-Objective Optimization”, [https://digitalcommons.odu.edu/gradposters2022\\_sciences/2/](https://digitalcommons.odu.edu/gradposters2022_sciences/2/), 2022.
- [3] J. J. Bisognano and G. A. Krafft, “Multipass Beam Breakup in the CEBAF Superconducting Linac”, in *Proc. LINAC’86*, Stanford, CA, USA, Jun. 1986, paper TH3-9, pp. 452-454.
- [4] Dario Pellegrini, “Beam Dynamic Studies in Recirculating Machines”, École Polytechnique Fédérale de Lausanne, 2016. doi:10.5075/epfl-thesis-6981
- [5] A. Slowik, H. Kwasnicka, “Evolutionary algorithms and their applications to engineering problems”, *Neural Computational & their Applications to Engineering Problems*, vol. 32, pp. 12363-12379, 2020. doi:10.1007/s00521-020-04832-8
- [6] K. Deb, “A Fast and Elitist Multi-objective Genetic Algorithm: NSGA-II”, *IEEE Transactions on Evolutionary Computation*, vol. 6, pp. 182-197, 2002. doi:10.1109/4235.996017
- [7] J. Blank, K. Deb, “Pymoo: Multi-Objective Optimization in Python”, *IEEE Access*, vol. 8, pp. 89497-89509, 2020. doi:10.1109/ACCESS.2020.2990567
- [8] S. A. Bogacz, “Challenges and Opportunities of Energy Recovering Linacs”, LAL Seminar, Orsay, 2017.
- [9] R. Marler and J. Arora, “Survey of multi-objective optimization methods for engineering”, *Structural and Multidisciplinary Optimization*, vol. 26, pp. 369-395, 2004. doi:10.1007/s00158-003-0368-6
- [10] I. Neththikumara, R. M. Bodenstein, S. A. Bogacz, T. Satogata, and A. Vandenhoeke, “An Evolutionary Algorithm Approach to Multi-Pass ERL Optics Design”, in *Proc. IPAC’21*, Campinas, Brazil, May 2021, pp. 3610-3613. doi:10.18429/JACoW-IPAC2021-WEPAB383